Structural Design of UAV Semi-Monoque Composite Wing

M. R. A. Hutagalung, [a] A. A. Latif, [a] H. A. Israr, [a*]

[a] Aeronautics Laboratory, Faculty of Mechanical Engineering,
Universiti Teknologi Malaysia,
81310 Skudai, Johor Darul Ta'zim.

Graphical Abstract
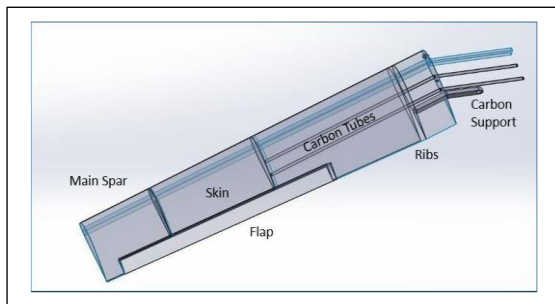
Abstract

This paper presents an analysis through simulation study of the structural design of a composite UAV wing. The semi-monoque structure consists of one main mono-spar, 4 major ribs, carbon tubes and a flap. The internal structures have been designed to promote better flight and structural performances. Wing loading calculations were done based on the parameters given under regulations of FAR Part 23: Airworthiness Standards. From these wing loading calculations, the value is then imported into Finite Element Method software, Abaqus for structural analysis. Composite failure criteria that are used are Tsai-Hill and Tsai-Wu. The final UAV wing design acquired a Tsai-Hill value of 0.1020 and Tsai-Wu value of 0.09851, which are both less than 1, conclusively the structures are safe to be fabricated and to be experimented with a wind tunnel for further validation. Through this study, it is found that decreasing the number of layers and changing the orientations play a significant role in the strength and overall weight of the UAV wings as desired.

Introduction

An unmanned aerial vehicle or also known as UAV is an aircraft that does not require a human pilot to be on board. UAVs can be flown either autonomously based on a pre-programmed flight plan as well as through a more sophisticated dynamic automation or by a pilot on the ground. UAVs play an important role in many fields including the military as well as defence sector, global positioning, mapping as well as homeland security [1]. In contrast, there seems to be a boom in the research of UAVs in terms of aerodynamics and structures in the early 2000s, ever since its introduction in the early 19th century. This could explain that the UAV technology has matured over the years and manufacturing costs has become economically feasible [2].

Universiti Teknologi Malaysia (UTM), in collaboration with Unmanned System Technology Sdn. Bhd. (UST) is designing a medium range-lightweight UAV weighing 40 kilograms under the Consolidated Advanced Model for Aeronautical Research (CAMAR) project as can be seen in Figure 1. Meanwhile, the wing structure is one of the most important aspects of the UAV. Without a proper wing design, the structural performance could be disturbed and optimum performance of the aerial vehicle could not be achieved. Structural performances of the wings must be studied to obtain maximum loading distribution before it buckles or fails under flight loads [3]. In aviation, it can be seen that the structural components of a UAV wing are similar to the ones that are on an aircraft [4].
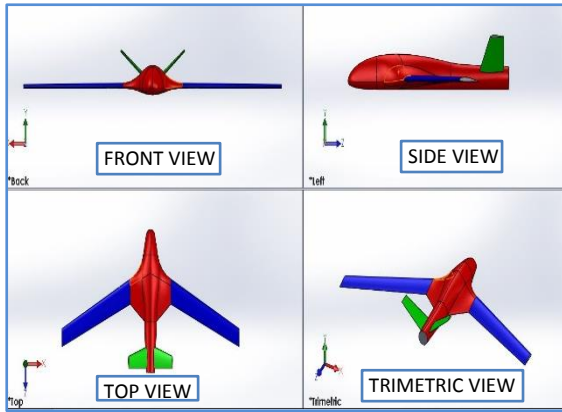
Figure 1: Four viewpoints of CAMAR UAV

The UAV wing structural members are proposed to carry a load and to oppose stresses acted upon it [5]. A semi-monoque structure as shown in Figure 2 has numerous amount of advantages against a monocoque structure including the ability of the skin to transfer and distribute all the loadings from the wings towards the internal structures to withstand an extremely high amount of loading before negatively impacted over a period of time [6].
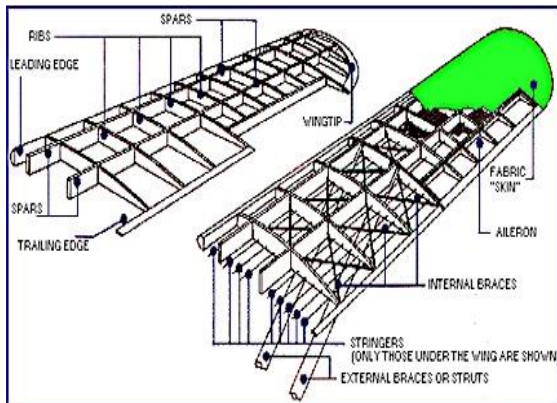
Figure 2: Semi-monoque UAV fixed wing structural components nomenclature [4]

Finite element method is a numerical solution towards a structural analysis problem. The application of computational mathematics can be used to solve UAV wing structural determination. It is a more practical solution when compared to experimental method due to the fact that it would be more economically feasible and optimizations can be performed according to desired iterations [7]. Numerous papers had been published regarding the finite element modelling (FEM) of a UAV wing. This includes the paper presented by Mazhar and Khan [8], who came up with the approach towards the structural design methodology for a UAV wing, through the use of Abaqus software, to study the stiffness and strength of the said wing. Apart from that, Sullivan

and Lacy [9] describes the design and implementation of a series of optimizations to measure the static and dynamic characteristics of a composite wing on a UAV. Jagdale *et al.* [10] provides a multidisciplinary approach to study the stresses developed during flight loads on a UAV wing and also discusses methods to optimize the composite layup as well as orientation of the UAV wing structures.

Nevertheless, limited studies are found in the open literature which used FEM to fully design a semi-monoque wing for small scale of UAV like CAMAR. Therefore, in this paper a structural design of a semi-monoque composite wing using FEM for CAMAR UAV will be carried out and discussed in the following sections.

FINITE ELEMENT METHODS: A NUMERICAL SOLUTION

Structural analysis of CAMAR UAV wing in this study have been carried out using Abaqus software. Before developing the numerical modelling, it is important to acknowledge the suitable failure criterion that can be used to simulate the performance of composite wing. Moreover, the aerodynamics loadings that CAMAR UAV will be experienced during flight also need to be determined. This is important in order to choose the appropriate materials, airfoil and wing configurations.

Composite Failure Theory Criterion

Many airframe structures currently are comprising more than 80% advanced composites due to its ideal weight to strength ratio [11].

Sodzi [12] describes the commonly used composite failure criteria in aircraft structural analysis. The main concern to study structural strength of the composite UAV wing would be Tsai-Hill Maximum Distortional Energy Theory and Tsai-Wu Strength Tensor Theory.

To further elaborate in detail, Tsai-Hill Maximum Distortional Energy Theory encompasses the metallic yielding theory of structures and assumes that there are interactions between stresses. In Tsai-Hill's Theory, yielding occurs when:

$$\frac{(F_1{}^2 - F_1 F_2)}{(F_L{}^Y)^2} + \frac{F_2{}^2}{(F_T{}^Y)^2} + \frac{F_{12}{}^2}{(F_{LT}{}^{SU})^2} = 1$$

Whereby;

$$
\begin{aligned}
F_1 &= F_L{}^{UT} \text{ or } F_L{}^{UC} \\
F_2 &= F_T{}^{UT} \text{ or } F_T{}^{UC} \\
F_{12} &= F_{LT}{}^{SU}
\end{aligned}
$$

T = Transverse direction.
Y = Yield stress or strain.
L = Longitudinal direction.
LT = Long transverse direction.
SU = Ultimate shear strain or stress.
UT = Ultimate tension.
UC = Ultimate compression.

In addition, Tsai-Wu Strength Tensor Theory applies when the composite panel is subjected to transformation with interaction between the stresses. Failure occurs when:

$$
\begin{aligned}
&(F_1\sigma_1 + F_2\sigma_2 + F_3\sigma_3 + F_4\sigma_4 + F_5\sigma_5 + F_6\sigma_6) \\
&+ \\
&(F_{11}\sigma_1{}^2 + F_{22}\sigma_2{}^2 + F_{33}\sigma_3{}^2 + F_{44}\sigma_4{}^2 + F_{55}\sigma_5{}^2 \\
&\qquad + F_{66}\sigma_6{}^2) \\
&+ \\
&(2F_{12}\sigma_1\sigma_2 + 2F_{13}\sigma_1\sigma_3 + 2F_{23}\sigma_2\sigma_3) \\
&\geq \\
&1
\end{aligned}
$$

It has to be known that the values for F_{11}, F_{12} and F_{23} can be found whilst conducting the simulation. While σ_1 to σ_6 are principle stresses throughout the lamina. τ is denoted as shear strengths in three planes of symmetry that are assumed to have the same magnitude on all planes. The coefficient of the orthotropic Tsai-Wu failure criterion would be:

$$
\begin{aligned}
F_1 &= \frac{1}{\sigma_{1T}} - \frac{1}{\sigma_{1C}} & F_{11} &= \frac{1}{\sigma_{1T}\sigma_{1C}} \\
F_2 &= \frac{1}{\sigma_{2T}} - \frac{1}{\sigma_{2C}} & F_{22} &= \frac{1}{\sigma_{2T}\sigma_{2C}} \\
F_3 &= \frac{1}{\sigma_{3T}} - \frac{1}{\sigma_{3C}} & F_{33} &= \frac{1}{\sigma_{3T}\sigma_{3C}} \\
F_{44} &= \frac{1}{\tau_{23}{}^2} & F_{55} &= \frac{1}{\tau_{31}{}^2} \\
F_{66} &= \frac{1}{\tau_{12}{}^2} & F_4 &= F_5 = F_6 = 0
\end{aligned}
$$

Wing Loading Distribution

Perkins *et al.* [13] claims that the aerodynamics forces and moments on the body of a UAV are due to two basic sources, which are the pressure distribution and shear stress distribution over the body surface. For the simplicity of the problem, shear stress distribution over the body surface is neglected, which provides meaning that all loads on the UAV are assumed to come from the lift forces generated over the wings as shown in Figure 3.

In addition, the concept of a sweptback wing is to be represented by a flat plate with the identical platform dimensions and twist distribution on both sides of the wings. A lifting line appears to exist as the linear line acts upon at 90-degree angle to the quarter chord line of the wing [14]. It is essential to evaluate the wing loading distribution to understand the loading contributions over the wing surface. Mainly, wing loadings are categorized as span-wise and also chord-wise lift distribution.
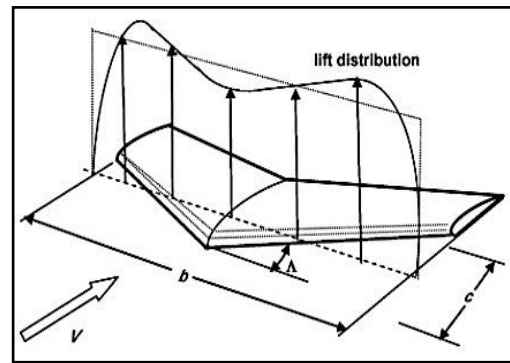
Figure 3: The lift distribution of a sweptback wing on a UAV [14]

Span-Wise Loading Distribution

Perry [15] promotes that pure Schrenk's Method is one of the ways to approximate the span-wise lift distribution. Basically, the plane of the wing is drawn with semi-span along the x-axis and chord on the y-axis. Then, a quadrant of an ellipse, whose area is equal to the area of the wing span is drawn. Furthermore, a curve joining the midpoints of the planform and the elliptical quadrant is drawn to visualize the total lift distribution of the half-span wing as shown in Figure 4. The steps to perform Schrenk's Method is highlighted in the next passage:

1. Divide the half span into 47 sections composed by fuselage, wing root, flap and wing tip.

2. Calculate:

$$\sqrt{1 - \left(\frac{2y}{b}\right)^2} \text{ for each station.}$$

3. Compute:

$$C_y = \frac{4S\sqrt{1 - \left(\frac{2y}{b}\right)^2}}{\pi b c}.$$

4. Calculate:

$$C_{cl} = \frac{4S\sqrt{1 - \left(\frac{2y}{b}\right)^2}}{2\pi b} + \frac{c}{2}.$$

5. Calculate local section lift for unity:

$$(C_L = 1) \; c_l = C_L(c_{la}) = C_L \frac{ccl}{\bar{c}}.$$

6. Calculate maximum local section lift:

$$(C_L = 1.364) \; cl_{Max} = C_L(cla) = C_L \frac{ccl}{\bar{c}}.$$

7. Compute:

$$(ccl_{Max}\Delta y)_n = \frac{c(clmax)n + c(clmax)n+1}{2} \; 2 \; [y_{n+1} - y_n].$$

8. Calculate:

$$L_n = = \frac{c(clmax)n}{\sum(cclmax\Delta y)n} \times n \times \frac{W}{2} \times g$$
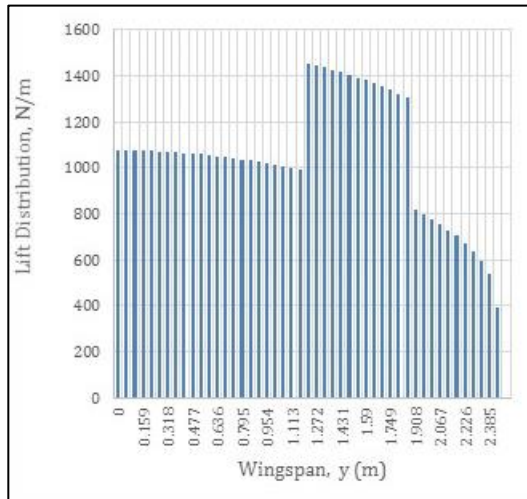
Figure 4: Graph of span-wise lift distribution with aileron effect

Chord-Wise Loading Distribution

Pressure distribution in the chord-wise direction is computed using the software called "XFOIL". XFOIL is an interactive program for the design and analysis of subsonic isolated aerofoils. Given the coordinates specifying the shape of a 2-dimensional aerofoil, the software can calculate the pressure distribution on the surface of the wings in chord-wise direction. The chord is divided into 23 divisions for simplicity of the case, with 0.041m distance in between each division that would make up x/c to 1, whereby c is 0.541m which is the root chord.
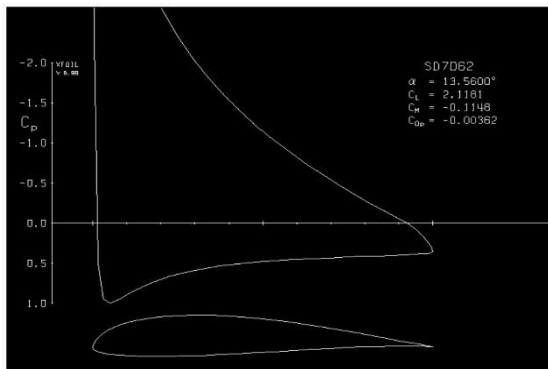
Figure 5: Pressure distribution in chord-wise direction of the CAMAR UAV wing

From the computations in Figure 5, the highest loading regardless at span-wise or chord-wise was chosen to be as the loading input. This is due to the fact that it is of high concern that this wing structure is able to withstand the highest load acted upon it whilst in flight. Knowing the coefficient of pressure, length of chord, and percentage of area, thus the highest load acted on wing is [1450*0.32]/(0.1*0.547) = 8140.35 Pa = 8140.35 N/m^2 to be used for Abaqus. It is concluded that the chord-wise lift distribution with 8140.35 N/m^2 is most significant when compared to the span-wise lift distribution of 1452.40 N/m^2.

Manoeuvre Envelope And Gust Loading

Flight envelope (Figure 6) and gust loading (Figure 7) studies are crucial to obtain the wing loading distribution in order to analyse the maximum loading condition that can be endured by the UAV. The variation of loadings that were calculated are C_L vs α, C_D vs C_L, C_T vs C_L, C_{Z_A} vs C_L, C_{L_X} vs C_L and C_{L_Z} vs C_L. Manoeuvre envelope or V-n diagram is the limitation of the environment where it is guaranteed for the UAV to be working as desired at CG_{Max}, CG_{Min}, CG_{Aft}, and CG_{Fwd}.
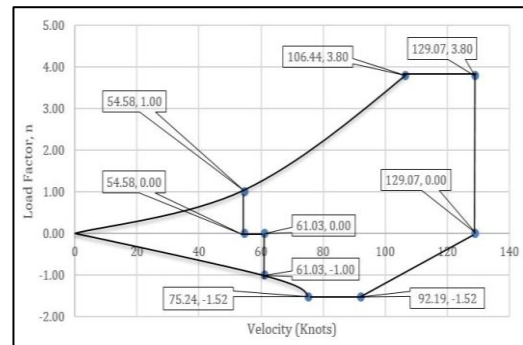
Figure 6: Graph of manoeuvre envelope for maximum CG case
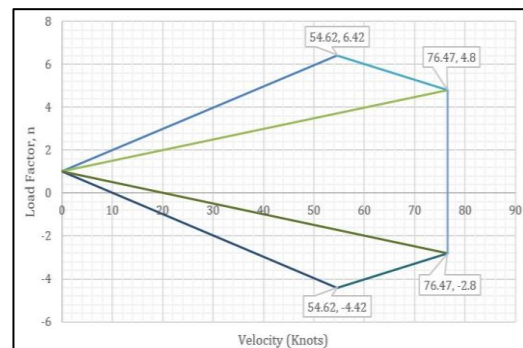
Figure 7: Graph of gust envelope for maximum CG condition

THE MODELLING OF THE UAV WING

Through the use of Computer Aided Design (CAD) software, SolidWorks 2014, the CAMAR UAV wing is designed. The design specification has prior constraints for instance, the aerofoil of the wings SD7062 and its wingspan have been pre-determined, thus reasonable measures are taken to ensure the best optimum design was considered to produce a UAV wing that could withstand the loadings for a prolonged period of time throughout its life cycle. The essential parameters of CAMAR UAV wing are listed in Table 1. To further optimize the structural design of the wing is by designing the internal structures and configurations of the wings.

Table 1: Essential Parameters of The UAV Wing

Components	Characteristics	Value
Wing	Chord Length (Root)	0.55m
	Chord Length (Tip)	0.39m
	Length of Half Span	2.5m
	Sweep Angle	24.95°
	Anhedral Angle	1.61°
	Wingspan, b	5.00m
Flap	Chord Length (Root)	0.0914m
	Chord Length (Tip)	0.0824m
	Length of Flap	1.0256m

Aerofoil Selection

The shape of the aerofoil plays an enormous role in the formation of the internal structures of the UAV. This is due to the fact that the aerofoil decides the shape of the wing ribs. The aerofoil SD7062 (Figure 8) was pre-selected because of its excellent performance for high payload UAVs at high lift and low drag configurations with low to high speed manoeuvres. The aerofoil has maximum thickness at 14% at quarter chord, maximum camber of 3.5% at 38.8% chord, stall angle at 15°, maximum coefficient of lift, C_{Lmax} of 1.6680 and lift curve slope, $C_{L\alpha}$ of 5.4010.
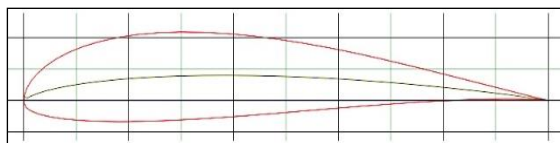
Figure 8: Shape of the SD 7062 aerofoil

Wing Configurations

The UAV wing design is a semi-monoque structure thus it has internal structures that would help to damp the loadings towards the wing skin. The components that would account the internal structures are a mono-spar, 5 leading edge ribs, 5

trailing edge ribs, carbon tubes, carbon support and the wing skin as shown in Figure 9.

The geometrical modelling of the wing structural components was designed using SolidWorks 2014, and then the 3-dimensional model was imported to Abaqus software for numerical simulation. However, since the wing was assumed to be symmetrical on both sides, the left side and the right side of the wing, only half of the wing span model is used in the numerical analysis and this have caused the reduction of computing time for the analysis to be completed [16].
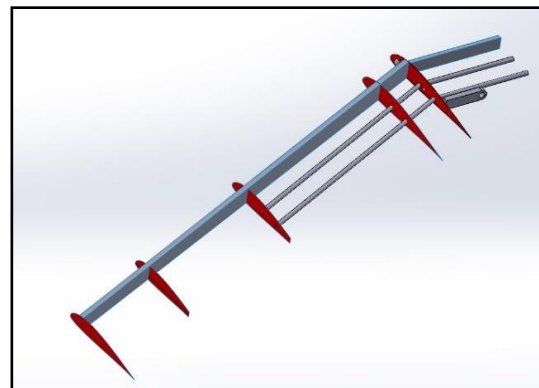
Figure 9: The internal structures of the CAMAR UAV wing

Material Selection

The major structural components of the wing were made of composite materials, which provides a great strength to weight ratio to the overall structure of the UAV wing except for fasteners, which provide support to attach the wings to the fuselage, bolts and also nuts. The main composite material used in the study would be carbon fibre with epoxy resin and carbon fibre braided with epoxy resin as the matrix. The characteristics of the composite material is tabulated in Table 2 and Table3.

Table 2: Material properties of the CAMAR UAV

Material	E_1 (GPa)	E_2 (GPa)	G_{12} (GPa)	V_{12}	P (Kg/m³)
Carbon Fibre Fabric (With Epoxy)	70	70	5	0.1	1600
Carbon Fibre Braided (With Epoxy)	34	34	3	0.4	1550

As the baseline of the research, the laminate design used for the skin of the wing as well as the flaps is carbon fibre fabric with stocking sequence of $[0_2, 45, -45, 0_{1/2}]_s$ with 9 layers. The total thickness of the component would be 0.002286m.

Meanwhile, The laminate design used for the 5 leading edge and 5 trailing edge ribs is 6 layers carbon fibre fabric with stacking sequence of [45, 0, 0]$_s$. The total thickness of the component would be 0.001524m.

Table 3: Elastic Properties of the composite materials for Abaqus simulation

Material	X_T (MPa)	X_C (MPa)	Y_T (MPa)	Y_C (MPa)	S (MPa)
Carbon Fibre Fabric (With Epoxy)	600	570	600	570	90
Carbon Fibre Braided (With Epoxy)	640	320	28.2	148.4	39.7

Furthermore, the laminate design used for the spar of the wing is also carbon fibre fabric with 15 layers of stacking sequence of [0, 45, 45, 0, 45, 0, 0, 45, 0, 0, 45, 0, 45, 45, 0]. Finally, the laminate design used for tubes support of the wing is carbon fibre braided with 6 layers stacking sequence of [45, 0, 0]$_s$. The total thickness of the component would be 0.001524m. From these baseline values, optimizations have been performed to acquire the most desired configurations that will be beneficial towards the ability for the UAV wing to execute to its preferred functions as determined in the preliminary design.

Meshing Of the UAV Wing Structural Components

According to Lee, Y. [17], meshing is formed through nodes, which are connected to form elements such that no elements overlap and the entire object is covered. In Lee's method, a square grid with the same spacing as the desired element size is superimposed on the object. The cells are visited in a columnar manner from left to right, and within the same column, from bottom to top. Within a cell, the points are sorted in ascending x-coordinates. Points having the same x-coordinate are sorted in ascending y- coordinates. The points are visited in turn. For each point, neighbouring points are found so as to form the nodes of a good quadrilateral failing which, a triangle is formed. All of the components use the meshing generation which are Quad-Dominated and automatic structured meshing as shown in Figure 10.

Given the large scale of the mode and nature of the structures, shell elements were used to represent the components with S4R four-noded shell elements coded in Abaqus as it is highly

effective as well as it could reduce computational time and running costs in the long run. A total of 289,642 elements were generated for the analysis.
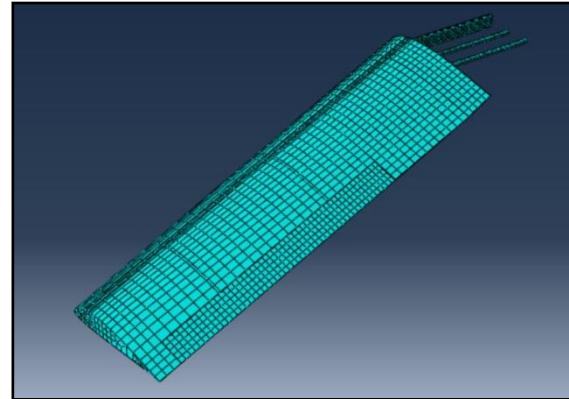
Figure 10: Meshing of the overall UAV wing assembly

Boundary Condition

The present work is aimed at utilizing the current finite element method for investigating complex composite structure criteria of the wing structure. With that, boundary conditions are necessary to define how the site specific model interacts with the entire environmental process. It also reflects the results of the simulation on the real world working condition. Without a proper boundary condition that is set onto the system, the reliability of the data would not be sufficient and valid for the real world application [18]. The boundary condition for the analysis is set on the points where the UAV wing is attached to the fuselage at the point of assembly when they are already interlocking with each other. The boundary condition that is set up is "Encastre" where the fuselage is assumed to be stiff enough to handle all the loadings acted upon it after being transferred from the wings. The surface condition is set up in Abaqus where it can only move along U3 while U1 and U would be 0, and they cannot rotate around UR_1, UR_2, and UR_3. As all degrees of freedom were set to zero at root as shown in Figure 11.
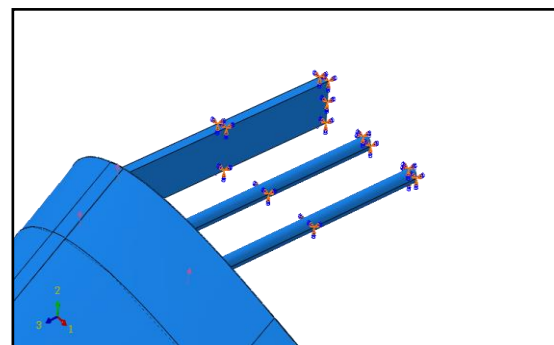
Figure 11: Boundary condition on the overall UAV wing assembly (Root)

The wing loading of the system has been calculated prior, whereby the span-wise loading is calculated through pure Schrenk method, and chord-wise loading distribution is replicated on the body of the wing after the point of boundary condition is set up on the system. The replication is done to the exact extent onto how the wings would reflect during the loadings that have been calculated earlier including fuselage and flap effect in terms of pressure. As highlighted in red in Figure 12, the loading value of 8140.35 N/m^2 is uniformly distributed across the top half and bottom half of the wing skin, with the direction going perpendicular outwards from the structure. The main issues to be studied would be the composite failure criterion, deflection and weight.
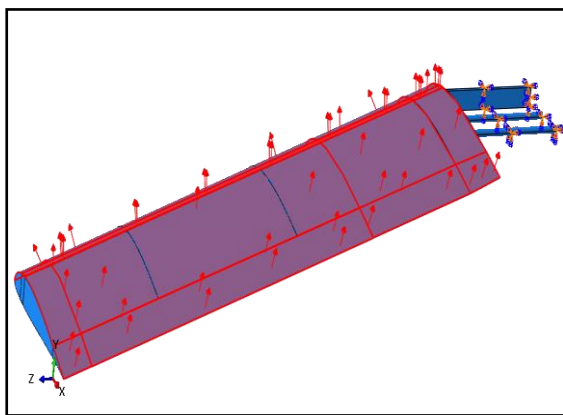
Figure 12: Loading Conditions On The Overall UAV Wing Assembly

RESULTS AND DISCUSSION

As mentioned earlier, Tsai-Hill and Tsai-Wu failure criteria of composite structures are being focussed as well as the deflection of the wing and finally the mass of the UAV wing. From the first simulation, the results have reached initial expectations and objectives.

The baseline simulation provides Tsai-Hill value of 0.1806 (Figure 13) as well as Tsai-Wu value of 0.1734 (Figure 14). Both showed a promise that the UAV wing is much capable of handling the loadings acted upon it as both are less than 1, which brings meaning that they do not fail. In fact, it is expected that the point of which the maximum value of implication towards the strength of the system would happen, occur at the root rib of the UAV wing, at the wing to fuselage attachment mechanism.

If the UAV wing design is computed to be of high deflection, thus optimizations are needed to be done to decrease this value alongside with the

other parameters at play. The maximum deflection of the UAV wing design is recorded at 1.780 mm, which happens at the wing tip as shown in Figure 15. A high deflection means that it would disturb the flight performance, thus reducing the battery management system of the UAV ending with a shorter range and shorter endurance. This is indeed an equally good deflection value as the deflection is 0.0712 % of the overall wing span. However, the deflection of the UAV wing is not limited during the pre-conceptual phase. Thus, this value is acceptable for the simulation as it is a stiff structure that could handle the loadings.
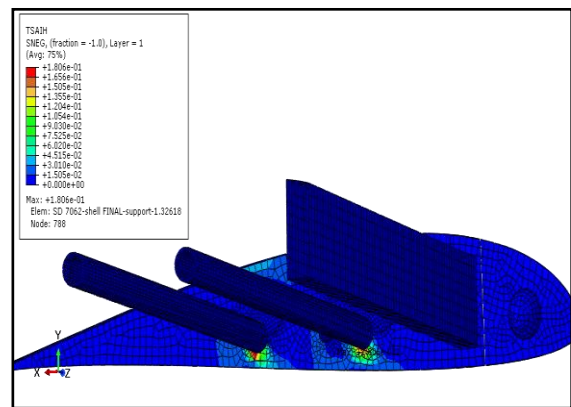
Figure 13: Tsai-hill failure criterion results
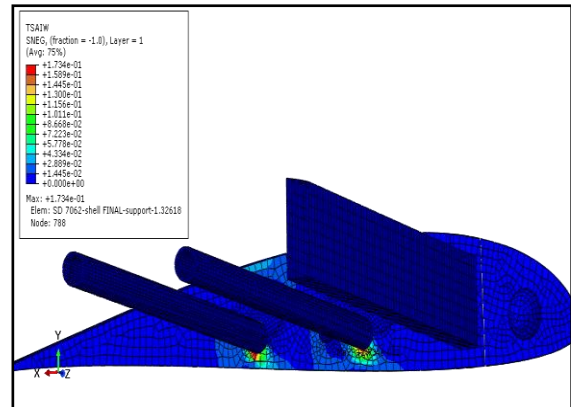
Figure 14: Tsai-wu failure criterion results
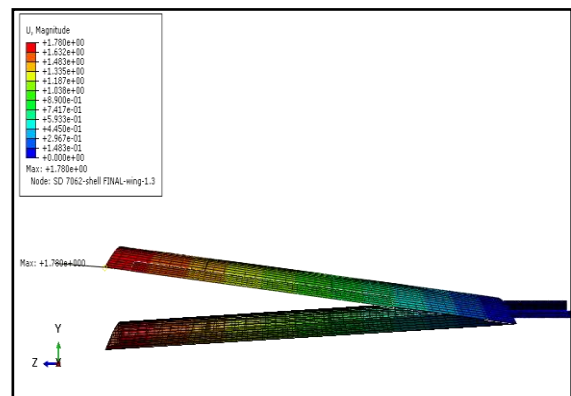
Figure 15: Maximum deflection of CAMAR UAV wing

Weight plays a major role in the overall UAV wing design. A less heavy wing would mean that the UAV could carry more payload and perform its functions. The maximum weight of the UAV obtained from the current design is 7.11195 kilograms. Whereby, the UAV is just half the span. A full wingspan UAV that is a total up of 5 meters long would be acquiring a total weight value of 14.2239 kilograms. 14.2239 kilograms weight of the wings alone account of about 35.56% of the overall weight of the UAV itself.

Optimizations

Based on the initial results, it is found that the UAV wing design is strong enough to handle the loadings acted upon it. Thus, to further strengthen the structure, it would be required to increase the thickness of the root rib so that it would contain the loadings. It can be seen that introduction of another 2 layers from 6 to 8 layers of carbon fibre fabric with orientation of 0 degrees, the thickened structure indeed affects the overall value of Tsai-Hill and Tsai-Wu of the UAV wing design. From the first optimization process, the Tsai-Hill value decreased to 0.1020 (Figure 16), while the Tsai-Wu value decreased to 0.09847 (Figure 17). The deflection is recorded to be declining at 0.8520 mm (Figure 18) but the overall mass of the UAV wing has increased to 7.12677 kilograms as shown in Figure 19.
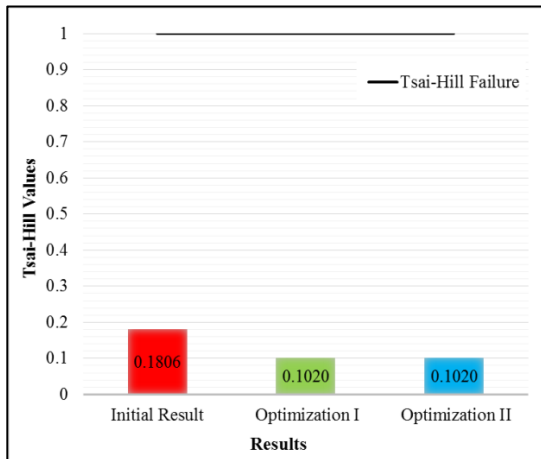
Figure 16: Breakdown of Tsai-Hill values after optimizations

After further analysis and discussion, it is concluded that the deflection values are of no issue, but the weight needs to be reduced. It is decided to reduce the thickness of the main spar, which involves much of the mass properties through analysis. From the number of 15 layers, it was reduced to just 11 layers while maintaining the same properties of the selected material. From

the second optimization process, the Tsai-Hill value maintains at 0.1020 (Figure 16) meanwhile the Tsai-Wu value increases to 0.09851 (Figure 17). At the same time, the deflection surges to 0.8526mm (Figure 18) but the mass of the UAV wing drops to just 6.7021 kilograms as plotted in Figure 19.
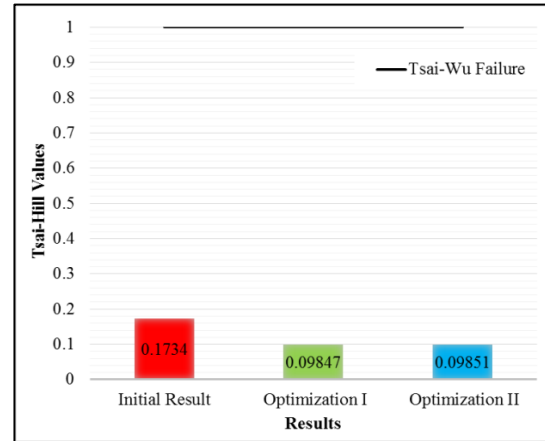
Figure 17: Breakdown of Tsai-Wu values after optimizations
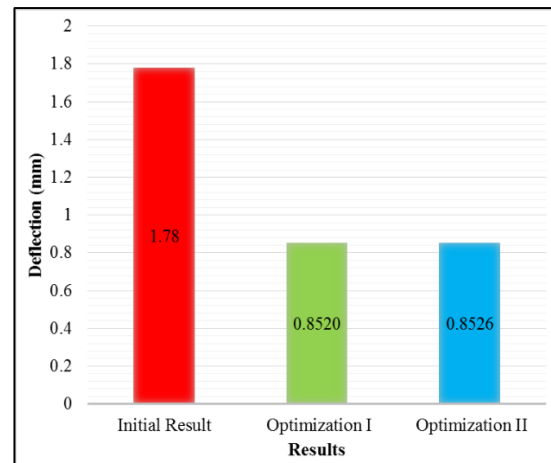
Figure 18: Breakdown of deflection after optimizations
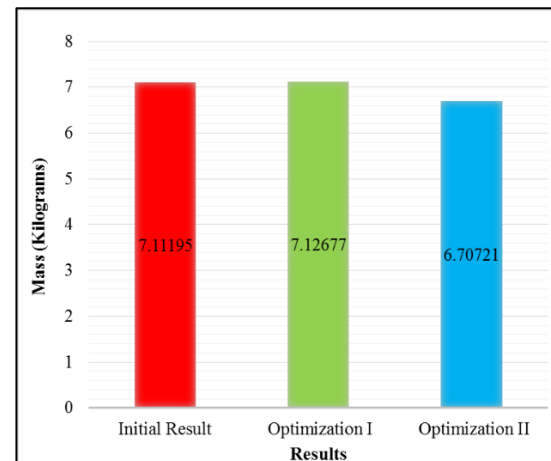
Figure 19: Breakdown of mass values after optimizations

CONCLUSION

The aim of this study is to examine the structural design of a semi-monoque composite wing for CAMAR UAV using numerical model. The developed model based on the desired design shows the capability to estimate the maximum deflection, weight and the stiffness of the wing by comparing with Tsai-Hill and Tsai-Wu criteria. In addition, the developed model also allows the optimization process of the CAMAR UAV wing design to be done easily in order to have the best configurations at the minimum weight.

The optimization of the thickening the root rib and reducing the thickness of the main spar is a success in maintaining a good strength to weight ratio as the UAV wing design is still stiff enough to conquer the loadings acted upon it. It can be seen that after optimization have been done on the UAV wing, the value of Tsai Hill decreased to 0.1020, which is desired, and the value of Tsai-Wu also decreased to 0.09851. On top of that, the value of deflection also decreased from 1.780 mm to 0.8526 mm. The slight decrease on both Tsai-Wu and deflection values of the UAV wing design is anticipated, as the justification is that the mass is managed to be decreased from 7.11195 kilograms to 6.70721 kilograms. The decrease of about 5.79714% is crucial towards the structural property of the UAV.

Nevertheless, the results obtained in this study is just an approximation. Thus, it is necessary to perform fabrication of the CAMAR UAV wing that is designed and conduct experimental testing in order to validate the results obtained in this study.

ACKNOWLEDGEMENTS

REFERENCES

[1] *Jagdale, V., Viana, F., Haftka, R. And Ifju, P. 2009. Conceptual design of a bendable uav wing considering aerodynamic and structural performance. AIAA 2010-2761.*

[2] *Federal Aviation Administration (FAA). 2012. Aviation maintenance technician handbook – Airframe (FAA-H-8083-31), Volume 1, Aircraft Structures. 46-48.*

[3] *Blyenburgh, P. 1999. UAVs: An overview. air & space europe, Volume 1. 43-47*

[4] *Gudmundsson, S. 2013. General aviation aircraft design. chapter 9: the anatomy of the aircraft wing, Volume 1. Butterworth Heinemann. 301-398.*

[5] *Ainsworth, J., Collier, C., Yarrington, P., Lucking, R. And Locke, J. 2010. Airframe wing-box preliminary design and weight prediction. Society of Allied Weight Engineers. SAWE. 40-41.*

[6] *Anderson, J. 2011. Fundamentals of aerodynamics. chapter 7: wing loading. McGraw-Hill Higher Education, 5th Edition. 726-732.*

[7] *Reytier, T., Bes, C., Marechal, P., Bianciardi, M. And Santgerma, A. 2012. Generation of correlated stress time histories from continuous turbulence power spectral density for fatigue analysis of aircraft structures. International Journal of Fatigue. 147-152.*

[8] *Mazhar, F. And Khan, A. 2010. Structural design of a uav wing using finite element method. 51st AIAA/ASME/ASCE/AHS/ASC Structures, Structural Dynamics, And Materials Conference, AIAA 2010-3099.*

[9] *Sullivan, R., Rohani, M., Lacy, T. And Alday, N. 2006. Structural testing of an ultralight uav composite wing. 47th AIAA/ASME/ASCE/AHS/ASC Structures, Structural Dynamics, And Materials Conference, AIAA 2006-1870.*

[10] *Jagdale, V., Stanford, B., Patil, A. And Ifju, P. 2009. Multidisciplinary shape and layup optimization of a bendable composite uav wing. AIAA 2009-1067.*

[11] *Federal Aviation Administration (FAA). 2012. Aviation maintenance technician handbook – Airframe (FAA-H-8083-31), Volume 2. 10-34.*

[12] *Sodzi, P. 2009. Damage tolerant wing-fuselage integration structural design. Cranfield University. PhD Thesis. 122-127.*

[13] *Perkins, D. And Hage, E. 1949. Airplane performance, stability and control. Chapter 4: Aircraft Performance. Wiley Publications. 1st Edition. 358-376.*

[14] *Sforza, P. 2014. Commercial airplane design principle. Appendix c: Airfoil and wing theory analysis. Butterworth Heinemann. Volume 1. 447-559.*

[15] *Perry, J. 1950. Aircraft structures. Chapter 3: Wing configurations. Dover Publications, Inc. 1st Edition. 322-353.*

[16] *Schaeffer, D. And Golubitsky, M. 1979. Boundary conditions and mode jumping in the buckling of a rectangular plate. Communications In Mathematical Physics. Spinger Publications. 209-236.*

[17] *Lee, Y. 1983. Automatic finite element generation based on constructive solid geometry. Phd Thesis. University of Leeds, United Kingdom.*